

Discovery of Potent and Selective Inhibitors of the Mammalian Target of Rapamycin (mTOR) Kinase

Pawel Nowak,^{*,†} Derek C. Cole,[†] Natasja Brooijmans,[§] Matthew G. Bursavich,[†] Kevin J. Curran,[†] John W. Ellingboe,[†] James J. Gibbons,[‡] Irwin Hollander,[‡] YongBo Hu,[§] Joshua Kaplan,[†] David J. Malwitz,[†] Lourdes Toral-Barza,[‡] Jeroen C. Verheijen,[†] Arie Zask,[†] Wei-Guo Zhang,[‡] and Ker Yu[‡]

[†]Chemical Sciences and [‡]Discovery Oncology and [§]Structural Biology, Wyeth Research, 401 N. Middletown Road, Pearl River, New York 10965

Received June 23, 2009

The mammalian target of rapamycin (mTOR) is a central regulator of cell growth, metabolism, and angiogenesis and an emerging target in cancer research. High throughput screening (HTS) of our compound collection led to the identification of 3-(4-morpholin-4-yl-1-piperidin-4-yl)-1*H*-pyrazolo[3,4-*d*]pyrimidin-6-yl)phenol (**5a**), a modestly potent and nonselective inhibitor of mTOR and phosphoinositide 3-kinase (PI3K). Optimization of compound **5a**, employing an mTOR homology model based on an X-ray crystal structure of closely related PI3K γ led to the discovery of 6-(1*H*-indol-5-yl)-4-morpholin-4-yl-1-[1-(pyridin-3-ylmethyl)piperidin-4-yl]-1*H*-pyrazolo[3,4-*d*]pyrimidine (**5u**), a potent and selective mTOR inhibitor (mTOR IC₅₀ = 9 nM; PI3K α IC₅₀ = 1962 nM). Compound **5u** selectively inhibited cellular biomarker of mTORC1 (P-S6K, P-4EBP1) and mTORC2 (P-AKT S473) over the biomarker of PI3K/PDK1 (P-AKT T308) and did not inhibit PI3K-related kinases (PIKKs) in cellular assays. These pyrazolopyrimidines represent an exciting new series of mTOR-selective inhibitors with potential for development for cancer therapy.

Introduction

The mammalian target of rapamycin (mTOR^a) is an unconventional high molecular weight serine/threonine protein kinase that regulates cell growth, proliferation, metabolism, and angiogenesis.^{1–5} mTOR is the founding member of the PI3K-related kinase (PIKK) family⁶ that also includes DNA-PK, ATM, ATR, and SMG-1. The PIKKs collectively play important and diverse roles in cell growth and surveillance of the genome and transcriptome. The catalytic sites of the PIKK family are similar to that of PI3K but differ significantly from the rest of the human kinome. mTOR primarily resides in two functional multiprotein complexes, mTOR complex 1 (mTORC1) and mTOR complex 2 (mTORC2), governing subcellular functions and/or substrate specificity. mTORC1 is a key regulator of cellular translation, while mTORC2 is anticipated to regulate the AKT survival

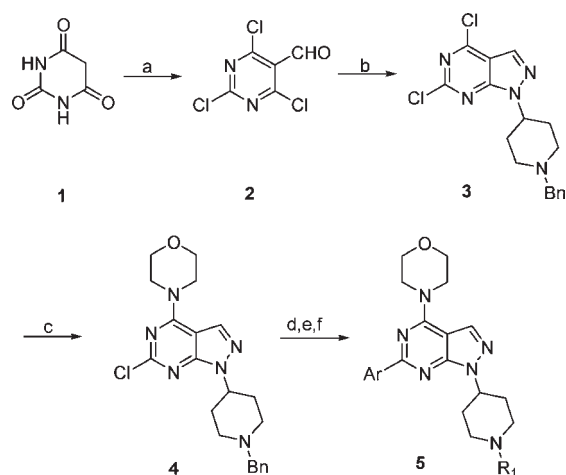
pathway and cytoskeletal network in human cells. mTORC1 and mTORC2 are critical mediators of the PI3K/AKT and Ras/MAPK signaling pathways that are frequently deregulated in human tumors.^{7–9}

Rapamycins (rapamycin and its analogs) are allosteric inhibitors that bind (in complex with FKBP12) to mTOR at the FKBP12-rapamycin binding domain (FRB domain) adjacent to the catalytic site of mTOR.^{10,11} These agents are used clinically for treating a subset of tumors.^{12–14} However, only the FRB domain of mTORC1 is inhibited by the rapamycin–FKBP12 complex while that of mTORC2 is insensitive to these inhibitors.^{15,16} Inhibition of mTORC1 by the rapamycins can also induce feedback activation of PI3K and ERK/MAPK in some settings.^{7,8,17} Therefore, although the rapalogs have validated mTOR clinically as a cancer target, their molecular mechanism of action does not fully exploit the antitumor potential of mTOR targeting in cancer. Small molecule ATP-competitive inhibitors of mTOR kinase should provide global inhibition of both mTORC1 and mTORC2 and hence minimize the feedback activation of PI3K signaling (via inhibition of the AKT pathway) to achieve more robust antitumor efficacy. The PI3K/mTOR pathway has been a subject of widespread and intense drug discovery efforts for a number of years and potent dual/pan-PI3K inhibitors have been reported,^{18–20} but only recently have reports describing mTOR selective compounds appeared.^{21–24}

Herein, we report the identification, characterization, and hit-to-lead optimization of a series of pyrazolopyrimidine mTOR kinase inhibitors exemplified by 4-(6-(1*H*-indol-5-yl)-1-(1-(pyridin-3-ylmethyl)piperidin-4-yl)-1*H*-pyrazolo[3,4-*d*]pyrimidin-4-yl)morpholine (**5u**). This small molecule lead (MW = 495, clogP = 2.1) has low nanomolar mTOR enzyme inhibitory activity, inhibits signaling functions of both

*To whom correspondence should be addressed. Phone: 845 602-4303. Fax: 845 602-5561. E-mail: nowakp@wyeth.com.

^aAbbreviations: mTOR, mammalian target of rapamycin; mTORC1, mammalian target of rapamycin complex 1; HTS, high-throughput screening; PI3K, phosphoinositide 3-kinase; PIKK, phosphoinositide 3-kinase related kinases; DNA-PK, DNA-dependent protein kinase; ATM, ataxia-telangiectasia mutated; ATR, ataxia-telangiectasia and Rad3-related; SMG-1, suppressor of morphogenesis in genitalia-1; Ras, rat sarcoma; MAPK, mitogen-activated protein kinase; FRB, FKBP12-rapamycin binding; ERK, extracellular signal-regulated kinase; DELFIA, dissociation-enhanced lanthanide fluorescent immunoassay; PRKCN, protein kinase C, NU; CLK1, CDC-like kinase 1; STK25, serine/threonine kinase 25; JAK2, Janus kinase 2; AMPK, AMP-activated protein kinase; PAK2, P21-activated kinase 2; CSK, c-src tyrosine kinase; FGFR1, fibroblast growth factor receptor 1; MST4, mammalian sterile twenty-like 4; TEK, TEK tyrosine kinase, endothelial; NTRK2, neurotrophic tyrosine kinase receptor type 2; PAK7, P21(CDKN1A)-activated kinase 7; SGK1, serum and glucocorticoid-inducible kinase-like kinase; HWT, 17-hydroxywortmannin; Rapa, rapamycin.

Scheme 1^a

^a Reagents and conditions: (a) POCl₃, DMF, reflux, 60%; (b) 1-benzyl-4-hydrazinylpiperidine dihydrochloride, Et₃N, EtOH, -78 to 0°C, 82%; (c) morpholine, EtOH, 61%; (d) ArB(OH)₂ or ArB(OCMe₂)₂, Pd(PPh₃)₄, Na₂CO₃, dioxane, water, 100°C; (e) H₂, Pd(OH)₂/C (10%), MeOH; (f) R₂COCl, Et₃N, THF or R₂CHO, NaBH₃CN, AcOH (cat.), MeOH.

mTORC1 and mTORC2 complexes in cellular setting, and is selective over PI3K α and other kinases.

Chemistry

The synthesis of **5a** and related compounds begins with treatment of barbituric acid (**1**) with phosphorus oxychloride (POCl₃) in dimethylformamide, resulting in formation of 2,4,6-trichloropyrimidine, which undergoes formylation leading to aldehyde **2** (Scheme 1). Reaction with substituted hydrazine produces the dichloropyrazolopyrimidine **3**. The 4-chloro substituent on dichloropyrazolopyrimidines **3** is selectively displaced by morpholine, leading to **4**. Finally, Suzuki coupling with boronic acid derivatives gives the target compounds **5**. In cases where the piperidinyl substitution was varied, the benzyl protecting group is removed by hydrogenation and the resulting secondary amine acylated or reductively alkylated (steps e and f). Compounds **5a–v** were assayed for inhibitory activity against mTOR (dissociation-enhanced lanthanide fluorescent immunoassay) and PI3K isoforms (fluorescence polarization assay).

Results and Discussion

An mTOR inhibitor high-throughput screen (HTS) led to the identification of compound **5a**, a promising “leadlike” starting point for further optimization because of its favorable properties: low MW (297), clogP (1.86), high ligand efficiency²⁵ (0.42), low LELP²⁶ (clogP/(ligand efficiency) = 4.4), and submicromolar potency (IC₅₀ = 215 nM). However, compound **5a** was 6-fold more potent for PI3K α than mTOR kinase and alerted us to a potential hurdle of achieving selectivity versus this closely related member of PI3K family of kinases.

In order to better understand the binding of pyrazolopyrimidins to the mTOR binding site, we have constructed an mTOR binding model based on an X-ray crystal structure of related PI3K γ kinase. The catalytic sites of mTOR and PI3K α differ only by two amino acid residues within a radius of 3 Å around **5a**, namely, Trp2239 to Val850 and Leu2354 to Phe930, respectively (Figure 1). Both these residues are near

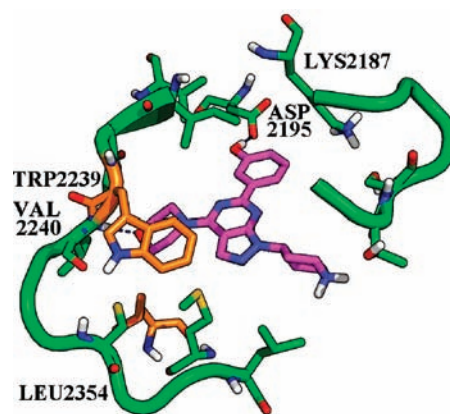


Figure 1. Putative binding mode of **5a** with the mTOR homology model. In this model, the morpholine of **5a** forms a key hinge-region hydrogen bond with the backbone of Val2240. At the rear of the binding pocket, Asp2195 is shown making a second key hydrogen bond to the phenol of **5a**. Residues within a 3 Å radius of **5a** that are conserved between the mTOR active site and PI3K α are shown in green and include the catalytic Lys2187. The only two residues that change (highlighted in orange) are Trp2239 and Leu2354. The core forms hydrophobic contacts with Ile2163 and Leu2185 above the plane of the inhibitor and with Met2345 and Ile2356 below the plane of the inhibitor (not shown for clarity).

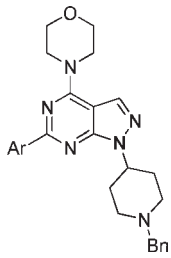
Table 1. Enzyme Inhibition Data for **5a–f** against mTOR and PI3K α ^a

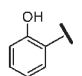
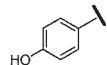
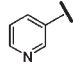
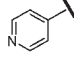
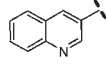
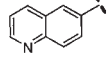
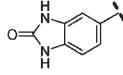
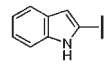
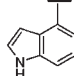
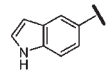
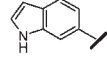
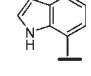
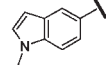
Comp	R ₁	mTOR	PI3K α
		IC ₅₀ [nM] [*]	IC ₅₀ [nM] [*]
5a	H	215	36
5b		49	69
5c		4	50
5d		6	86
5e		78	31
5f		10	47

^a The asterisk (*) indicates that IC₅₀ determinations are the mean of two to three independent measurements with standard error of <20%.

the morpholine but do not make specific hydrogen bonding interactions with the compound.

We began modifying our lead **5a** by derivatizing the piperidine NH group. The acetylpiperidine derivative **5b** had

Table 2. Enzyme Inhibition Data for **5g**–**s** against mTOR and PI3K α ^a


Comp	Ar	mTOR	PI3K α
		IC ₅₀ [nM] [*]	IC ₅₀ [nM] [*]
5g		1265	3565
5h		170	720
5i		695	244
5j		7300	2766
5k		120	6000
5l		5950	466
5m		195	4394
5n		130	1112
5o		145	238
5p		88	1008
5q		230	1272
5r		380	520
5s		575	5190

^aThe asterisk (*) indicates that IC₅₀ determinations are the mean of two to three independent measurements with standard error of <20%.

5-fold improved activity and almost equal potency in the two enzymes (see Table 1). Introduction of the benzoyl (**5e**) and nicotinyl (**5d**) groups led to compounds with low nanomolar

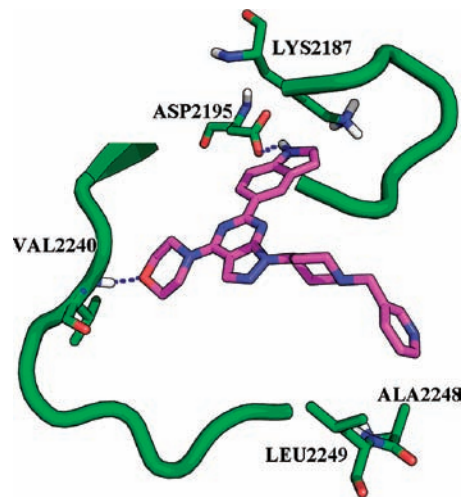
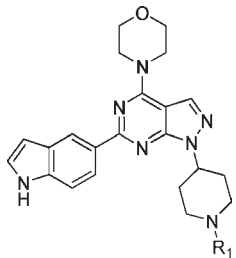


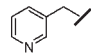
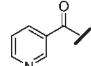
Figure 2. Predicted binding mode of **5u** with the mTOR homology model. The predicted binding mode of **5u** with mTOR shows the hydrogen bonding interaction of the morpholine to Val2240 and the indole-NH to Asp2195. The pyridin-3-ylmethyl tailpiece of **5u** in the front of the binding site interacts with a region that contains Leu2249 and Ala2248 in mTOR. The corresponding residues in PI3K α are Met858 and Gln859, respectively.

activity and, for the first time, more than 10-fold selectivity versus PI3K α . The corresponding benzyl (**5e**) and 3-pyridylmethyl (**5f**) analogues were somewhat less potent and selective.

Simultaneous with the optimization of the piperidine substitution, the benzyl analogue **5e** was chosen as a starting point to explore the SAR of the pyrazolopyrimidine aryl substituent. Moving the phenolic hydroxyl group to the 2- or 4-position of the aryl ring (**5g** and **5h**) led to a loss in activity (see Table 2) which is explained by the loss of the key hydrogen bond to Asp2195 (Figure 1). The metabolic liability associated with the presence of a phenol group, as evidenced by short rat hepatocyte clearance half-life ($t_{1/2} = 13$ min for **5e**), prompted a search for suitable replacements. In the pyridyl and quinolonyl series (**5i**–**l**), compounds having a nitrogen H-bond acceptor in the 3- position showed modest potency. The 5-benzimidazolonyl derivative **5m** was modestly active and > 20-fold selective over PI3K α . Further investigation of analogous indole substituents (**5n**–**r**) led to the identification of the 5-indolyl derivative **5p**, which was equipotent with the original phenol **5e** and had > 10-fold selectivity. The *N*-Me indole **5s** was almost 6-fold less active, suggesting that either the N–H of **5p** is involved in the same hydrogen bonding interaction as the phenol with Asp2195, as predicted by modeling (Figure 2), or the *N*-Me results in a steric clash with the protein, resulting in the lower activity of **5s**.

Having found that the indole substituent leads to potent and selective mTOR inhibitors, we further explored piperidine substituents (Table 3). Compound **5t**, having an unsubstituted piperidine group, had only modest potency; however, substitution of the piperidine with pyridin-3-ylmethyl (**5u**) and nicotinyl (**5v**) groups gave, as expected (cf. **5d**, and **5f**, Table 1), compounds of excellent activity and highly amplified selectivity vs PI3K α (> 1000-fold). The selectivity increases associated with modifications of groups in positions 1 and 6 of the pyrazolopyrimidine appear to be cumulative. This selectivity enhancement may be a result of accessing the more hydrophobic region in mTOR (Ala2248 and Leu2249 versus Met858 and Gln859 in PI3K α).

Table 3. Enzyme Inhibition Data for **5t–v** against mTOR and PI3K α ^a


Comp	R ₁	mTOR IC ₅₀ [nM] [*]	PI3K α IC ₅₀ [nM] [*]
5t	H	170	1310
5u		9	1962
5v		4	5870

^aThe asterisk (*) indicates that IC₅₀ determinations are the mean of two to three independent measurements with standard error of <20%.

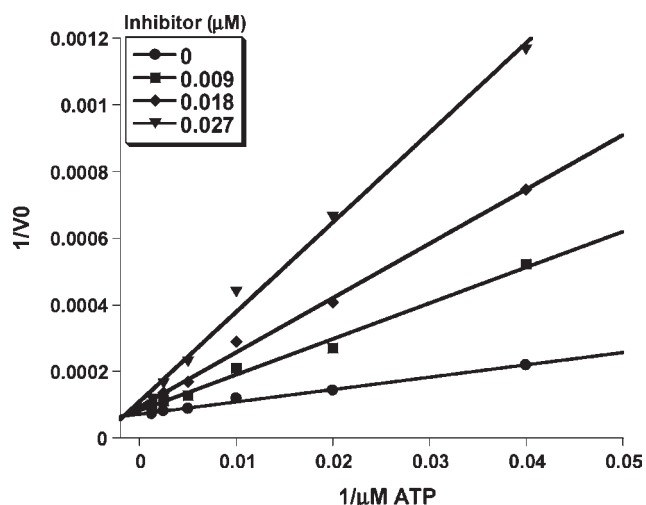


Figure 3. ATP competitive inhibition of mTOR kinase activity. Compound **5u** was assayed in an inhibitor versus ATP matrix competition. The initial enzyme rate (V_0) against 0, 0.009, 0.018, 0.027 μM **5u** at various concentrations of ATP was measured to generate the double-reciprocal plot.

Compound **5u** was the earliest example in the “indole” series to display excellent selectivity over PI3K α , and hence, it was the most fully characterized. In the Invitrogen kinase panel²⁷ compound **5u** had less than 50% inhibition at 2 μM against 219 of 231 kinases and had modest activity (50–85% inhibition at 2 μM) against 12 kinases, namely, PRKCN, CLK1, STK25, JAK2, AMPK, PAK2, CSK, FGFR1, MST4, TEK, NTRK2, PAK7, and SGKL.

The ATP-competitive nature of inhibition of compound **5u** was confirmed in a Lineweaver–Burk double-reciprocal dose–response plot (Figure 3) of the mTOR enzyme rates against the ATP concentration.

A498 renal cancer cells treated with **5u** or rapamycin showed a distinctive biochemical profile (Figure 4).

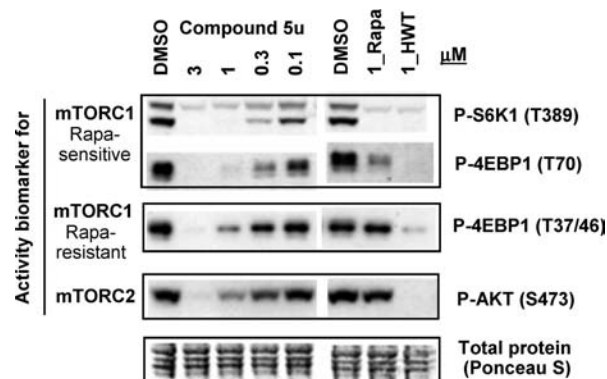


Figure 4. Inhibition of cellular mTORC1 and mTORC2 signaling functions in actively proliferating cancer cells. Renal tumor A498 cells were treated in growth medium for 6 h with DMSO or the indicated concentrations of **5u** or 1 μM rapamycin (Rapa) or 17-hydroxywortmannin (HWT). Total cell lysates were prepared and subject to immunoblotting with antibodies against P-S6K1(T389), P-4EBP1(T70), P-4EBP1(T36/47), P-AKT(S473). The blots were also stained with Ponceau S, a total protein dye, for sample loading control.

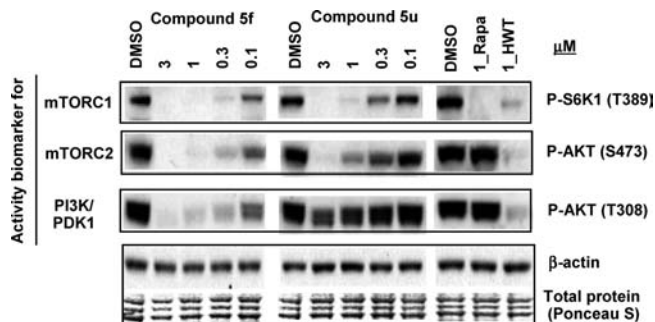


Figure 5. Selective targeting of mTOR versus PI3K in PTEN-negative cancer cells. U87MG glioma cells were treated in growth medium for 6 h with DMSO or the indicated concentrations of **5f** or **5u** or 1 μM rapamycin (Rapa) or 17-hydroxywortmannin (HWT). Total cell lysates were prepared and subject to immunoblotting with antibodies against P-S6K1 (T389), P-AKT (S473), and P-AKT (T308).

Rapamycin inhibited mTORC1 biomarkers P-S6K1(T389) and P-4EBP1(T70) but not the rapamycin-resistant mTORC1 biomarker P-4EBP1(T37/46) or the biomarker P-AKT(S473). In contrast, the global mTOR inhibitor **5u** inhibited both mTORC1 and mTORC2 biomarkers in a dose-dependent manner.

Treatment of PTEN-negative, PI3K/AKT-hyperactive U87MG glioma cells with **5u** selectively inhibited P-S6K-(T389) and P-AKT(S473) but not P-AKT(T308), an activity biomarker of PI3K/PDK1. In contrast, a nonselective inhibitor **5f** and the PI3K inhibitors HWT all indiscriminately inhibited P-AKT(S473) and P-AKT(T308) (Figure 5). Thus, both the biochemical and cellular results support **5u** as an ATP-competitive and selective inhibitor of mTOR kinase.

Conclusion

Through mTOR inhibitor HTS, we identified a “leadlike” small molecule inhibitor of mTOR kinase. The hit-to-lead optimization was guided by a PI3K γ based mTOR homology model and led to the identification of an indolopyrazolopyrimidine series, exemplified by 4-(6-(1*H*-indol-5-yl)-1-(1-(pyri-

din-3-ylmethyl)piperidin-4-yl)-1*H*-pyrazolo[3,4-*d*]pyrimidin-4-yl)morpholine (**5u**), a 9 nM ATP-competitive inhibitor of mTOR kinase with >200-fold selectivity over PI3K α , which showed only modest activity against 12 out of the 231 protein kinases. **5u** selectively inhibited mTOR over PI3K α and the related PIKK²¹ in cellular settings and inhibited proliferation of a panel of histologically diverse cancer cell lines.²¹ The results of continued optimization and in vivo efficacy studies of this promising series will be disclosed.

Experimental Methods

NMR spectra were recorded on a Bruker Avance 300 MHz spectrometer. All chemical shifts are reported in parts per million (δ) relative to tetramethylsilane. The following abbreviations are used to denote signal patterns: s = singlet, d = doublet, t = triplet, m = multiplet, and br = broad. The mass spectral data were determined on an Agilent 1100 series LC/MSD, and HRMS was carried out on a Bruker APEX II 9.4 T mass spectrometer. Silica gel flash chromatography was carried out on a Teledyne Isco, Inc. CombiFlash Companion using RediSep silica gel cartridges. Reverse phase HPLC purifications were performed on a Gilson preparative HPLC system controlled by Unipoint software using either Phenomenex Gemini 100 mm \times 21.2 mm or Waters Xterra Prep 5 μ M, 100 mm \times 19 mm C₁₈ columns and in a 10–90% acetonitrile in water solvent gradient with 0.02% TFA buffer or with 0.02% ammonium hydroxide buffer. The purity of all compounds was \geq 95%. The purity was analyzed using Agilent Technologies 1200 series LCMS with Agilent XDB-C18 30 mm \times 2.1 mm, 1.8 μ m particle size column: solvent gradient = 90% A at 0 min, 5% A at 2.6 min, 5% A at 3 min; solvent A = 0.05% modifier in water; solvent B = 0.05% modifier in ACN; flow rate 1 mL/min. Modifiers used were NH₄OH or HCO₂H.

1-Benzyl-4-hydrazinylpiperidine Dihydrochloride.²⁸ Benzoic hydrazide (5.47 g, 40.2 mmol) was dissolved in methanol (30 mL) and 1-benzylpiperidin-4-one (7.60 g, 40.2 mmol) added, and the solution was stirred for 1 h at 30 °C and for 4 h at 60 °C. The solution was cooled in an ice bath, and sodium borohydride (1.52 g, 40.2 mmol) was slowly added. After 2 h the solvent was evaporated and the residue was partitioned between chloroform (50 mL) and saturated sodium bicarbonate (50 mL). The chloroform fraction was separated, dried with magnesium sulfate, and concentrated giving yellow oil (20.0 g). Water (16 mL) and concentrated hydrochloric acid (28 mL) were added. The solution was stirred for 15 min and the residual chloroform removed. The aqueous solution was refluxed overnight and then cooled in an ice bath, and the precipitated benzoic acid was filtered off. The filtrate was concentrated (~20 mL volume), and ethanol (100 mL) was added. The solution was cooled, and white crystals were filtered off and washed with a small portion of ethanol followed by diethyl ether. The solid was dried in high vacuum overnight (5.30 g, 76%). Mp: 200 °C. ¹H NMR (300 MHz, DMSO-*d*₆): δ 11.19–11.04 (br s, 1H), 7.67–7.60 (m, 2H), 7.47–7.42 (m, 3H), 4.31–4.22 (m, 2H), 3.40–3.28 (m, 2H), 3.18–3.03 (m, 2H), 3.02–2.89 (m, 1H), 2.17–1.99 (m, 3H), 1.85–1.72 (m, 1H). ¹³C NMR (75 MHz, DMSO-*d*₆): δ 131.8, 131.7, 130.2, 130.3, 129.7, 129.0, 58.7, 53.8, 49.6, 46.2, 26.9, 24.0. IR: 2964, 2464, 1063, 1037 cm⁻¹. MS (ES+): *m/z* 206.2 [M + H]⁺ (100%). HRMS: *m/z* 206.16446, calcd [M + H]⁺ 206.16482, rel intens 100%, error -0.36 mAu.

2,4,6-Trichloropyrimidine-5-carbaldehyde (2).²⁹ Phosphorus oxychloride (46 mL) was added dropwise over 20 min to dimethylformamide cooled in an ice bath. The solution was stirred for further 20 min after, and barbituric acid (8.00 g, 62.4 mmol) was added in one portion. The solution was stirred for 1 h at room temperature, and then it was heated to 100 °C for 4 h. The solution was evaporated to half-volume, and while still warm it was poured onto ice (200 g). Water (200 mL) was

added, and the suspension was stirred for 15 min. The yellow precipitate was filtered off, dissolved in chloroform (200 mL), and washed with water. The solution was dried with magnesium sulfate and filtered through small silica pad with the aid of dichloromethane. The solvents were evaporated, and the residue was triturated with hexanes. White crystals were filtered off and dried in high vacuum (8.00 g, 60%). Mp: 130–132 °C. ¹H NMR (300 MHz, chloroform-*d*): δ 10.42 (s). ¹³C NMR (75 MHz, chloroform-*d*): δ 184.6, 164.1, 161.6, 122.9. IR: 2964, 1702, 1054, 1036 cm⁻¹. MS (ES-): *m/z* 211.8 [M]⁺ (23%), 209.8 [M]⁺ (26%), 192.8 (69%), 190.8 (100%). Anal. Calcd for C₅HCl₃N₂O: C 28.40; H 0.48; N 13.25. Found: C 28.51; H 0.77; N 13.28.

1-(1-Benzylpiperidin-4-yl)-4,6-dichloro-1*H*-pyrazolo[3,4-*d*]pyrimidine (3). 2,4,6-Trichloro-5-pyrimidinecarboxaldehyde (**2**) (5.00 g, 23.65 mmol) was dissolved in ethanol (100 mL). The solution was cooled to -78 °C and 1-benzyl-4-hydrazinylpiperidine dihydrochloride (4.12 g, 23.65 mmol) added followed by triethylamine (9.9 mL, 70.90 mmol). The solution was stirred at -78 °C for 0.5 h and then warmed up to 0 °C and stirred at this temperature for 1.5 h. Ethyl acetate (500 mL) and saturated sodium bicarbonate (100 mL) were added, and the organic phase was separated, dried with anhydrous magnesium sulfate, and concentrated (bath temperature of <15 °C). The residue was dissolved in ethyl acetate (100 mL), and the solution was filtered through a plug of silica gel followed by elution with more ethyl acetate (20 mL). Removal of solvent (rotovap bath temperature of <15 °C) gave a thick yellow oil (7.01 g, 82%) which was unstable at room temperature and was immediately used in the next step. Analytical sample was converted to hydrochloride salt by dissolution in ethanol followed by saturation with gaseous hydrogen chloride and removal of solvent. The sample was stable enough to collect analytical data. Mp >230 °C (dec). ¹H NMR (300 MHz, DMSO-*d*₆): δ 10.78 (br s, 1H), 8.61 (s, 1H), 7.65–7.59 (m, 2H), 7.51–7.46 (m, 3H), 5.12–5.02 (m, 1H), 4.32 (s, 2H), 3.53–3.43 (m, 2H), 3.61–3.21 (m, 2H), 2.59–2.46 (m, 2H), 2.21–2.12 (m, 2H). ¹³C NMR (75 MHz, DMSO-*d*₆): δ 155.3, 154.4, 153.9, 133.6, 131.8, 130.0, 129.8, 129.1, 113.2, 59.3, 52.2, 50.4, 28.3. IR: 3432, 1026 cm⁻¹. MS (ES+): *m/z* 362.1 [M + H]⁺ (100%), 364.1 [M + H]⁺ (48%). Anal. Calcd for C₁₇H₁₈Cl₃N₅·0.1EtOH: C 51.22; H 4.65; N 17.36. Found: C 51.58; H 4.28; N 16.87.

4-(1-(1-Benzylpiperidin-4-yl)-6-chloro-1*H*-pyrazolo[3,4-*d*]pyrimidin-4-yl)morpholine (4). 1-(1-Benzylpiperidin-4-yl)-4,6-dichloro-1*H*-pyrazolo[3,4-*d*]pyrimidine (**3**) (7.00 g 19.32 mmol) was dissolved in ethanol (100 mL). The solution was cooled to 0 °C, and morpholine (1.68 mL, 19.32 mmol) was added. The solution was stirred for 0.5 h at 0 °C and 0.5 h at room temperature, the solvent was evaporated, and the residue was dissolved in ethyl acetate (200 mL). The solution was washed with saturated sodium bicarbonate (50 mL), the insoluble particles were removed by filtration and the phases separated, and the organic solution was dried with magnesium sulfate. The solvents were evaporated, and the residue was redissolved in ethyl acetate (50 mL) and filtered through a small (5 g) pad of silica with ethyl acetate elution. The solvent was evaporated leaving thick oil. The oil was dissolved in diethyl ether (50 mL) which led to spontaneous crystallization. The yellow crystals were filtered off and dried in high vacuum overnight (7.98 g, 61%). Mp 144–146 °C. ¹H NMR (300 MHz, DMSO-*d*₆): δ 8.35 (s, 1H), 7.35–7.31 (m, 4H), 7.30–7.27 (m, 1H), 4.64–4.50 (m, 1H), 3.91–3.85 (m, 4H), 3.73–3.69 (m, 4H), 3.53 (s, 2H), 2.97–2.84 (m, 2H), 2.22–2.02 (m, 4H), 1.87–1.78 (m, 2H). ¹³C NMR (75 MHz, DMSO-*d*₆): δ 156.5, 156.0, 153.9, 138.4, 133.2, 128.5, 128.0, 126.7, 98.7, 65.6, 61.7, 53.8, 51.9, 45.8 (low intensity), 30.8. IR: 32954, 1554, 1305, 945 cm⁻¹. MS (ES+): *m/z* 413.2 [M + H]⁺ (100%). Anal. Calcd for C₂₁H₂₅ClN₆O: C 61.08; H 6.10; N 20.35. Found: C 60.98; H 5.94; N 20.33.

4-(1-(1-Benzylpiperidin-4-yl)-6-(1*H*-indol-5-yl)-1*H*-pyrazolo[3,4-*d*]pyrimidin-4-yl)morpholine (5p). 4-(1-(1-Benzylpiperidin-4-yl)-

6-chloro-1*H*-pyrazolo[3,4-*d*]pyrimidin-4-yl)morpholine (**4**) (1.30 g, 3.15 mmol) was dissolved in dioxane (5 mL). 1*H*-Indol-5-ylboronic acid (633 mg, 3.94 mmol) followed by tetrakis(triphenylphosphine)palladium(0) (273 mg, 0.24 mmol) and 2 M aqueous sodium carbonate (5 mL) was added. The solution was degassed with a stream of nitrogen, and it was heated in a microwave reactor for 3 min at 120 °C. The reaction mixture was partitioned between ethyl acetate (25 mL) and 1 M aqueous sodium hydroxide (25 mL), and the organic fraction was separated, dried with magnesium sulfate, and evaporated. The oily residue was purified by flash chromatography (gradient of ethyl acetate to ethyl acetate/methanol/triethylamine, 8:1:1). Removal of solvent and drying in high vacuum gave an off-white, amorphous solid (1.31 g, 90%). ¹H NMR (300 MHz, DMSO-*d*₆): δ 11.25 (s, 1H), 8.71 (s, 1H), 8.31–8.22 (m, 2H), 7.46 (d, *J* = 9.0 Hz, 1H), 7.41–7.23 (m, 6H), 6.57 (s, 1H), 4.90–4.86 (m, 1H), 4.07–3.98 (m, 4H), 3.83–3.76 (m, 4H), 3.56 (s, 2H), 3.02–2.94 (m, 2H), 2.31–2.13 (m, 4H), 1.96–1.85 (m, 2H). ¹³C NMR (75 MHz, DMSO-*d*₆): δ 160.7, 156.5, 154.6, 138.4, 137.2, 132.5, 128.8, 128.6, 128.0, 127.4, 126.8, 126.0, 121.6, 120.6, 110.8, 102.1, 98.4, 65.8, 61.8, 53.3, 52.1, 44.9 (low intensity), 31.0. IR 2928, 1580, 1065, 1030, 1005 cm⁻¹. MS (ESI): *m/e* 247.6 (7%), 494.3 [M + H]⁺ (100%). Anal. Calcd for C₂₉H₃₁N₇O·²/₃H₂O: C 68.89; H 6.45; N 19.39. Found: C 68.88; H 5.92; N 19.57.

4-(6-(1*H*-Indol-5-yl)-1-(piperidin-4-yl)-1*H*-pyrazolo[3,4-*d*]pyrimidin-4-yl)morpholine (5t**).** 4-(1-(1-Benzylpiperidin-4-yl)-6-(1*H*-indol-5-yl)-1*H*-pyrazolo[3,4-*d*]pyrimidin-4-yl)morpholine (**5p**) (1.00 g, 20.3 mmol) was dissolved in tetrahydrofuran–methanol (50 mL, 1:1). Palladium hydroxide (0.75 g, 20% on carbon) was added, and the solution was hydrogenated at atmospheric pressure overnight. The catalyst was filtered off on a Cellite pad, and the solvent was evaporated. The residue was purified by flash chromatography (gradient of dichloromethane to dichloromethane/methanol/triethylamine, 3:1:1). Removal of solvent and drying in high vacuum gave an off-white, amorphous solid (0.45 g, 55%). ¹H NMR (300 MHz, DMSO-*d*₆): δ 11.25 (s, 1H), 8.71 (s, 1H), 8.31–8.24 (m, 2H), 7.45 (d, *J* = 8.5 Hz, 1H), 7.39 (dd, *J* = 2.5, 2.5 Hz, 1H), 6.57 (s, 1H), 4.94–4.81 (m, 1H), 4.05–3.97 (m, 4H), 3.49–3.77 (m, 4H), 3.15–3.05 (m, 2H), 2.77–2.64 (m, 2H), 2.13–1.96 (m, 3H), 1.88–1.78 (m, 2H). ¹³C NMR (75 MHz, DMSO-*d*₆): δ 160.6, 156.5, 154.4, 137.3, 132.4, 128.9, 127.4, 126.0, 121.6, 120.6, 110.8, 102.1, 98.4, 65.9, 53.9, 45.3, 45.0 (low intensity), 32.5. IR: 3260, 2930, 1570 cm⁻¹. MS (ESI): *m/e* 404.2 [M + H]⁺ (100%). Anal. Calcd for C₂₂H₂₅N₇O·2H₂O: C, 60.12; H, 6.65; N, 22.31. Found: C 60.53; H 6.25; N 22.5.

General Procedures. Procedure A: Suzuki Coupling. The piperidine compound (0.25 mmol) was dissolved in dioxane (2 mL), and boronic acid (0.25 mmol) followed by tetrakis(triphenylphosphine)palladium(0) (28 mg, 0.025 mmol) and 2 M aqueous sodium carbonate (2 mL) was added. The solution was degassed with a stream of nitrogen, and it was heated in a microwave reactor for 3 min at 120 °C. The reaction mixture was partitioned between ethyl acetate (10 mL) and saturated aqueous sodium bicarbonate (10 mL). The organic fraction was separated, dried with anhydrous magnesium sulfate, and evaporated. The residue was purified by preparative HPLC.

Procedure B: Reductive Amination. The piperidine compound (0.25 mmol) was dissolved in methanol (10 mL), and 3-pyridinecarboxaldehyde (80 mg, 0.75 mmol) was added followed by sodium cyanoborohydride (62 mg, 1.00 mmol) and acetic acid (0.05 mL). The solution was stirred overnight. Solvent was evaporated, and the residue was partitioned between ethyl acetate (10 mL) and saturated aqueous sodium bicarbonate (10 mL). The organic fraction was separated, dried with anhydrous magnesium sulfate, and evaporated. The residue was purified by preparative HPLC.

Procedure C: Conversion to Amide. The piperidine compound (0.25 mmol) was dissolved in tetrahydrofuran (5 mL), and acid chloride (0.30 mmol) was added followed by triethylamine (0.09

mL, 0.60 mmol). The solution was stirred for 1 h. Ethyl acetate (10 mL) and saturated aqueous sodium bicarbonate (10 mL) were added, and the organic fraction was separated, dried with anhydrous magnesium sulfate, and evaporated. The residue was purified by preparative HPLC.

3-(4-Morpholin-4-yl-1-piperidin-4-yl-1*H*-pyrazolo[3,4-*d*]pyrimidin-6-yl)phenol (5a**).** This compound was prepared in an analogous manner to **5p** and **5v**, using 3-hydroxyphenylboronic acid instead of 1*H*-indol-5-ylboronic acid. Purification was by preparative reverse phase HPLC with 0.02% ammonium hydroxide buffer. ¹H NMR (300 MHz, DMSO-*d*₆): δ 9.57 (br s, 1H), 8.31–8.27 (m, 1H), 7.90–7.86 (m, 2H), 7.66–7.54 (m, 1H), 7.28 (dd, *J* = 8.0, 8.0 Hz, 1H), 6.90–6.84 (m, 1H), 4.93–4.80 (m, 1H), 4.03–3.69 (m, 8H), 3.18–3.03 (m, 2H), 2.79–2.65 (m, 2H), 2.14–1.78 (m, 4H). MS (ESI): *m/e* 381.2 [M + H]⁺ (100%). HRMS *m/z* 381.203 63, calcd [M + H]⁺ 381.203 35, rel intens 100%, error 0.28 mAmu.

3-[1-(1-Acetylpiperidin-4-yl)-4-morpholin-4-yl-1*H*-pyrazolo[3,4-*d*]pyrimidin-6-yl]phenol (5b**).** Procedure C was used. The piperidine substrate for procedure C was prepared in an analogous manner to **5p** and **5t**, using 3-hydroxyphenylboronic acid instead of 1*H*-indol-5-ylboronic acid. The product was purified by preparative reverse phase HPLC with 0.02% ammonium hydroxide buffer, giving an off-white amorphous solid. ¹H NMR (300 MHz, DMSO-*d*₆): δ 8.33–8.29 (m, 2H), 7.83–7.74 (m, 1H), 7.66–7.53 (m, 1H), 7.23–7.16 (m, 1H), 6.84–6.78 (m, 1H), 5.09–4.90 (m, 1H), 4.54–4.44 (m, 1H), 4.02–3.87 (m, 5H), 3.81–3.66 (m, 6H), 2.05 (s, 3H), 2.08–1.80 (m, 4H). MS (ESI): *m/e* 423.2 [M + H]⁺ (100%), (M + K)⁺ 461.2 (6%). HRMS *m/z* 423.213 69, calcd [M + H]⁺ 423.213 92, rel intens 100%, error 0.23 mAmu.

3-[1-(1-Benzoylpiperidin-4-yl)-4-morpholin-4-yl-1*H*-pyrazolo[3,4-*d*]pyrimidin-6-yl]phenol (5c**).** Procedure C was used. The chloro substrate for procedure C was prepared in an analogous manner to **5p** and **5t**, using 3-hydroxyphenylboronic acid instead of 1*H*-indol-5-ylboronic acid. The product was purified by preparative reverse phase HPLC with 0.02% ammonium hydroxide buffer, giving an off-white amorphous solid. ¹H NMR (300 MHz, DMSO-*d*₆): δ 9.55 (s, 1H), 8.34 (s, 1H), 7.94–7.87 (m, 2H), 7.48 (s, 5H), 7.29 (dd, *J* = 8.0, 8.0 Hz, 1H), 6.89 (dd, *J* = 2.0, 8.5 Hz, 1H), 5.19–5.04 (m, 1H), 4.74–4.55 (m, 4H), 4.06–3.97 (m, 5H), 3.21–3.03 (m, 1H), 2.20–1.87 (m, 5H). MS (ESI): *m/e* 485.2 [M + H]⁺ (100%). HRMS *m/z* 485.229 07, calcd [M + H]⁺ 485.229 57, rel intens 100%, error 0.50 mAmu.

3-{4-Morpholin-4-yl-1-[1-(pyridin-3-ylcarbonyl)piperidin-4-yl]-1*H*-pyrazolo[3,4-*d*]pyrimidin-6-yl}phenol (5d**).** Procedure C was used. The chloro substrate for procedure C was prepared in an analogous manner to **5p** and **5t**, using 3-hydroxyphenylboronic acid instead of 1*H*-indol-5-ylboronic acid. The product was purified by preparative reverse phase HPLC with 0.02% ammonium hydroxide buffer, giving an off-white amorphous solid. ¹H NMR (300 MHz, DMSO-*d*₆): δ 9.53 (s, 1H), 8.69–8.65 (m, 2H), 8.33 (s, 1H), 7.94–7.85 (m, 3H), 7.51 (dd, *J* = 4.5, 8.0 Hz, 1H), 7.28 (dd, 7.5, 7.5 Hz, 1H), 6.87 (dd, *J* = 3.5, 8.0 Hz, 1H), 5.17–5.07 (m, 1H), 4.68–4.57 (m, 1H), 4.04–3.97 (m, 4H), 3.82–3.75 (m, 4H), 3.25–3.11 (m, 3H), 2.33–1.85 (m, 4H). MS (ESI): *m/e* 157.0 (15%), 486.2 [M + H]⁺ (100%). HRMS *m/z* 486.224 47, calcd [M + H]⁺ 486.224 82, rel intens 100%, error 0.35.

3-[1-(1-Benzylpiperidin-4-yl)-4-morpholin-4-yl-1*H*-pyrazolo[3,4-*d*]pyrimidin-6-yl]phenol (5e**).** Procedure A was used. Purification was by preparative reverse phase HPLC with 0.02% ammonium hydroxide buffer, giving an off-white amorphous solid. ¹H NMR (300 MHz, DMSO-*d*₆): δ 9.51 (s, 1H), 8.30 (s, 1H), 7.89–7.84 (m, 2H), 7.38–7.32 (m, 4H), 6.89–6.85 (m, 1H), 4.83–4.74 (m, 1H), 4.03–3.96 (m, 4H), 3.81–3.76 (m, 4H), 3.57 (s, 2H), 3.02–2.94 (m, 2H), 2.27–2.15 (m, 4H), 1.96–1.85 (m, 2H). MS (ESI): *m/e* 413.2 (13%), 471.2 [M + H]⁺ (100%). HRMS *m/z* 471.251 07, calcd [M + H]⁺ 471.250 30, rel intens 100%, error 0.77 mAmu.

3-{4-Morpholin-4-yl-1-[1-(pyridin-3-ylmethyl)piperidin-4-yl]-1H-pyrazolo[3,4-d]pyrimidin-6-yl}phenol (5f). Procedure A was used. The piperidine substrate for procedure B was prepared in an analogous manner to **5p** and **5t**, using 3-hydroxyphenylboronic acid instead of 1H-indol-5-ylboronic acid. The product was purified by preparative reverse phase HPLC with 0.02% ammonium hydroxide buffer, giving an off-white amorphous solid. ¹H NMR (300 MHz, DMSO-*d*₆): δ 9.52 (s, 1H), 8.57–8.46 (m, 2H), 8.31 (s, 1H), 7.90–7.75 (m, 3H), 7.39 (dd, *J* = 4.5, 7.0 Hz, 1H), 7.27 (dd, *J* = 8.0, 8.0 Hz, 1H), 6.89–6.87 (m, 1H), 4.85–4.72 (m, 1H), 4.04 (m, 4H), 3.83 (m, 4H), 3.61 (s, 2H), 3.03–2.93 (m, 2H), 2.32–2.13 (m, 4H), 1.97–1.89 (m, 2H). MS (ESI): *m/e* 236.5 (5%), 472.2 [M + H]⁺ (100%). HRMS *m/z* 472.245 56, calcd [M + H]⁺ 472.245 55, rel intens 100%, error 0.03 mAmu.

2-[1-(1-Benzylpiperidin-4-yl)-4-morpholin-4-yl-1H-pyrazolo[3,4-d]pyrimidin-6-yl]phenol (5g). Procedure A was used. Purification was by preparative reverse phase HPLC with 0.02% TFA buffer, giving an off-white amorphous solid. ¹H NMR (300 MHz, DMSO-*d*₆): δ 13.46 (m, 1H), 9.73 (m, 1H), 8.48–8.41 (m, 2H), 7.59–7.35 (m, 5H), 6.98–6.90 (m, 2H), 6.56 (m, 1H), 5.11–4.98 (m, 1H), 4.46–4.34 (m, 2H), 4.02–3.93 (m, 4H), 3.85–3.75 (m, 4H), 3.60–3.23 (m, 4H), 2.47–2.11 (m, 4H). MS (ESI): *m/e* 471.2 [M + H]⁺ (100%). HRMS *m/z* 471.250 19, calcd [M + H]⁺ 471.250 30, rel intens 100%, error 0.11 mAmu.

4-[1-(1-Benzylpiperidin-4-yl)-4-morpholin-4-yl-1H-pyrazolo[3,4-d]pyrimidin-6-yl]phenol Trifluoroacetic Acid Salt (5h). Procedure A was used. Purification was by preparative reverse phase HPLC with 0.02% TFA buffer, giving an off-white amorphous solid. ¹H NMR (300 MHz, DMSO-*d*₆): δ 9.29 (br s, 1H), 8.34–8.27 (m, 3H), 7.59–7.46 (m, 5H), 6.89–6.82 (m, 2H), 5.17–5.02 (m, 1H), 4.46–4.33 (m, 2H), 4.03–3.91 (m, 4H), 3.82–3.72 (m, 4H), 3.62–3.23 (m, 4H), 2.49–2.10 (m, 4H). MS (ESI): *m/e* 471.2 [M + H]⁺ (100%). HRMS *m/z* 471.250 97, calcd [M + H]⁺ 471.250 30, rel intens 100%, error 0.67 mAmu.

1-(1-Benzylpiperidin-4-yl)-4-morpholin-4-yl-6-pyridin-3-yl-1H-pyrazolo[3,4-d]pyrimidine (5i). Procedure A was used. Purification was by preparative reverse phase HPLC with 0.02% TFA buffer, giving an off-white amorphous solid. ¹H NMR (300 MHz, DMSO-*d*₆): δ 9.95 (br s, 1H), 9.61 (s, 1H), 8.40 (s, 1H), 8.77–8.68 (m, 2H), 7.62–7.46 (m, 6H), 5.21–5.07 (m, 1H), 4.43–4.35 (m, 2H), 4.08–3.98 (m, 4H), 3.83–3.74 (m, 4H), 3.61–3.24 (m, 4H), 2.51–2.14 (m, 4H). MS (ESI): *m/e* 228.2 (29%), 456.2 [M + H]⁺ (100%). HRMS *m/z* 456.251 46, calcd [M + H]⁺ 456.250 64, rel intens 100%, error 0.82 mAmu.

1-(1-Benzylpiperidin-4-yl)-4-morpholin-4-yl-6-pyridin-4-yl-1H-pyrazolo[3,4-d]pyrimidine Trifluoroacetic Acid Salt (5j). Procedure A was used. Purification was by preparative reverse phase HPLC with 0.02% TFA buffer, giving an off-white amorphous solid. ¹H NMR (300 MHz, DMSO-*d*₆): δ 9.63 (br s, 1H), 8.77–8.73 (m, 2H), 8.43 (s, 1H), 8.34–8.30 (m, 2H), 7.57–7.49 (m, 5H), 5.20–5.09 (m, 1H), 4.17–4.35 (m, 2H), 4.07–3.98 (m, 4H), 3.92–3.47 (m, 6H), 2.39–2.10 (m, 4H). MS (ESI): *m/e* 228.6 (32%), 379.2 (17%), 456.2 [M + H]⁺ (100%). HRMS *m/z* 456.251 37, calcd [M + H]⁺ 456.250 64, rel intens 100%, error 0.73 mAmu.

3-[1-(1-Benzylpiperidin-4-yl)-4-morpholin-4-yl-1H-pyrazolo[3,4-d]pyrimidin-6-yl]quinoline Trifluoroacetic Acid Salt (5k). Procedure A was used. Purification was by preparative reverse phase HPLC with 0.02% TFA buffer, giving an off-white amorphous solid. ¹H NMR (300 MHz, DMSO-*d*₆): δ 9.94 (s, 1H), 9.30 (s, 1H), 8.42 (s, 1H), 8.14 (dd, *J* = 8.0, 21.5 Hz, 2H), 7.85 (dd, *J* = 7.5, 7.5 Hz, 1H), 7.7 (dd, *J* = 7.5, 7.5 Hz, 1H), 7.59–7.50 (m, 6H), 5.27–5.15 (m, 1H), 4.47–4.37 (m, 2H), 4.13–4.03 (m, 4H), 3.87–3.75 (m, 4H), 3.61–3.30 (m, 4H), 2.48–2.17 (m, 4H). MS (ESI): *m/e* 253.6 (62%), 506.3 [M + H]⁺ (100%). HRMS *m/z* 506.266 99, calcd [M + H]⁺ 506.266 29, rel intens 100%, error 0.70 mAmu.

6-[1-(1-Benzylpiperidin-4-yl)-4-(morpholin-4-yl)-1H-pyrazolo[3,4-d]pyrimidin-6-yl]quinoline Trifluoroacetic Acid Salt (5l). Procedure A was used. Purification was by preparative reverse phase HPLC with 0.02% TFA buffer, giving an off-white amorphous solid. ¹H NMR (300 MHz, DMSO-*d*₆): δ 9.71 (s, 1H), 9.08 (d, *J* = 2.0 Hz, 1H), 8.99 (dd, *J* = 1.5, 4.5 Hz, 1H), 8.86 (dd, *J* = 2.0, 9.0 Hz, 1H), 8.59 (d, *J* = 8.0 Hz, 1H), 8.42 (s, 1H), 8.15 (d, *J* = 7.5 Hz, 1H), 7.64 (dd, *J* = 4.0, 8.5 Hz, 1H), 7.60–7.49 (m, 5H), 2.29–5.15 (m, 1H), 4.45–4.38 (m, 2H), 4.14–4.02 (m, 4H), 3.87–3.76 (m, 4H), 3.63–3.53 (m, 2H), 3.46–3.31 (m, 2H), 2.53–2.35 (m, 2H), 2.30–2.18 (m, 2H). MS (ESI): *m/e* 253.6 (66%), 506.3 [M + H]⁺ (100%). HRMS *m/z* 506.267 21, calcd [M + H]⁺ 506.266 29, rel intens 100%, error 0.92.

5-[1-(1-Benzylpiperidin-4-yl)-4-morpholin-4-yl-1H-pyrazolo[3,4-d]pyrimidin-6-yl]-1,3-dihydro-2H-benzimidazol-2-one Trifluoroacetic Acid Salt (5m). Procedure A was used. Purification was by preparative reverse phase HPLC with 0.02% TFA buffer, giving an off-white amorphous solid. ¹H NMR (300 MHz, DMSO-*d*₆): δ 10.88 (s, 1H), 10.74 (s, 1H), 8.34 (s, 1H), 8.16 (dd, *J* = 1.5, 5.5 Hz, 1H), 8.0 (s, 1H), 7.59–7.46 (m, 5H), 7.0 (s, 1H), 5.20–5.03 (m, 1H), 4.45–4.35 (m, 2H), 4.05–3.94 (m, 4H), 3.84–3.74 (m, 4H), 3.60–3.25 (m, 4H), 2.48–2.11 (m, 4H). MS (ESI): *m/e* 511.2 [M + H]⁺ (100%). HRMS *m/z* 511.256 42, calcd [M + H]⁺ 511.256 45, rel intens 100%, error 0.03 mAmu.

1-(1-Benzylpiperidin-4-yl)-6-(1H-indol-2-yl)-4-morpholin-4-yl-1H-pyrazolo[3,4-d]pyrimidine (5n). Procedure A was used. Purification was by preparative reverse phase HPLC with 0.02% ammonium hydroxide buffer, giving an off-white amorphous solid. ¹H NMR (300 MHz, DMSO-*d*₆): δ 11.61 (s, 1H), 8.62–8.56 (m, 1H), 8.25–8.20 (m, 2H), 7.49–7.14 (m, 8H), 4.82–4.69 (m, 1H), 4.02–3.95 (m, 4H), 3.82–3.76 (m, 4H), 5.58 (s, 2H), 3.12–2.94 (m, 4H), 2.34–1.89 (m, 4H). MS (ESI): *m/e* 247.6 (7%), 494.3 [M + H]⁺ (100%). HRMS *m/z* 494.267 07, calcd [M + H]⁺ 494.266 29, rel intens 100%, error 0.78 mAmu.

1-(1-Benzylpiperidin-4-yl)-6-(1H-indol-4-yl)-4-morpholin-4-yl-1H-pyrazolo[3,4-d]pyrimidine Trifluoroacetic Acid Salt (5o). Procedure A was used. Purification was by preparative reverse phase HPLC with 0.02% TFA buffer, giving an off-white amorphous solid. ¹H NMR (300 MHz, DMSO-*d*₆): δ 11.29 (s, 1H), 9.68 (s, 1H), 8.37 (s, 1H), 8.18 (d, *J* = 7.0 Hz, 1H), 7.60–7.38 (m, 7H), 7.24–7.16 (1H), 6.56 (s, 1H), 5.22–5.10 (m, 1H), 4.46–4.37 (m, 2H), 4.08–3.98 (m, 4H), 3.85–3.75 (m, 4H), 3.60–3.51 (m, 2H), 2.52–2.33 (m, 2H), 2.30–2.17 (m, 4H). MS (ESI): *m/e* 247.6 (17%), 494.3 [M + H]⁺ (100%). HRMS *m/z* 494.266 35, calcd [M + H]⁺ 494.266 29, rel intens 100%, error 0.06.

1-(1-Benzylpiperidin-4-yl)-6-(1H-indol-6-yl)-4-morpholin-4-yl-1H-pyrazolo[3,4-d]pyrimidine Trifluoroacetic Acid Salt (5q). Procedure A was used. Purification was by preparative reverse phase HPLC with 0.02% TFA buffer, giving an off-white amorphous solid. ¹H NMR (300 MHz, DMSO-*d*₆): δ 11.29 (a, 1H), 9.71 (br s, 1H), 8.53 (s, 1H), 8.34 (s, 1H), 8.21 (dd, *J* = 1.5, 8.5 Hz, 1H), 7.64–7.46 (m, 7H), 6.48 (s, 1H), 5.23–5.09 (m, 1H), 4.49–4.36 (m, 2H), 4.09–3.98 (m, 4H), 3.86–3.77 (m, 4H), 3.75–3.50 (m, 2H), 2.57–2.32 (m, 4H), 2.30–2.15 (m, 2H). MS (ESI): *m/e* 247.6 (11%), 494.3 [M + H]⁺ (100%). HRMS *m/z* 494.265 80, calcd [M + H]⁺ 494.266 29, rel intens 100%, error 0.49 mAmu.

1-(1-Benzylpiperidin-4-yl)-6-(1H-indol-7-yl)-4-morpholin-4-yl-1H-pyrazolo[3,4-d]pyrimidine (5r). Procedure B was used. Purification was by preparative reverse phase HPLC with 0.02% ammonium hydroxide buffer, giving an off-white amorphous solid. ¹H NMR (300 MHz, DMSO-*d*₆): δ 11.14 (s, 1H), 9.95 (br s, 1H), 8.40 (s, 1H), 8.31 (d, *J* = 8.0 Hz, 1H), 7.45 (d, *J* = 8.0 Hz, 1H), 7.65–7.45 (m, 7H), 7.16 (dd, *J* = 7.0, 7.0 Hz, 1H), 6.60 (s, 1H), 5.47–5.34 (m, 1H), 4.47–4.38 (m, 2H), 4.08–4.00 (m, 4H), 3.85–3.78 (m, 4H), 3.62–3.30 (m, 4H), 2.49–2.16 (m, 4H). MS (ESI): *m/e* 494.3 [M + H]⁺ (100%). HRMS *m/z* 494.266 41, calcd [M + H]⁺ 494.266 29, rel intens 100%, error 0.12 mAmu.

1-(1-Benzylpiperidin-4-yl)-6-(1-methyl-1H-indol-5-yl)-4-morpholin-4-yl-1H-pyrazolo[3,4-d]pyrimidine (5s). Procedure A was

used. Purification was by preparative reverse phase HPLC with 0.02% ammonium hydroxide buffer, giving an off-white amorphous solid. ¹H NMR (300 MHz, DMSO-*d*₆): δ 8.71 (s, 1H), 8.32 (d, *J* = 9.5 Hz, 1H), 8.27 (s, 1H), 7.49 (d, *J* = 8.5 Hz, 1H), 7.40–7.31 (m, 5H), 7.31–7.24 (m, 1H), 6.57 (d, *J* = 3.0 Hz, 1H), 4.91–4.77 (m, 1H), 4.07–3.98 (m, 4H), 3.83 (s, 3H), 3.84–3.75 (m, 4H), 3.57 (s, 2H), 3.04–2.93 (m, 2H), 2.32–2.13 (m, 4H), 1.96–1.85 (m, 2H). MS (ESI): *m/e* 254.6 (13%), 508.3 [M + H]⁺ (100%). HRMS *m/z* 508.281 44, calcd [M + H]⁺ 508.281 94, rel intens 100%, error 0.50 mAmu.

6-(1*H*-Indol-5-yl)-4-morpholin-4-yl-1-[1-(pyridin-3-ylmethyl)-piperidin-4-yl]-1*H*-pyrazolo[3,4-*d*]pyrimidine Trifluoroacetic Acid Salt (5u). Procedure B was used. Purification was by preparative reverse phase HPLC with 0.02% TFA buffer, giving an off-white amorphous solid. ¹H NMR (300 MHz, DMSO-*d*₆): δ 1.85 (brs, 1H), 11.35 (s, 1H), 9.19 (s, 1H), 8.97 (d, *J* = 5.4 Hz, 1H), 8.77 (d, *J* = 8.5 Hz, 1H), 8.74 (s, 1H), 8.32 (s, 1H), 8.30 (dd, *J* = 7.5, 0.5 Hz, 1H), 8.06 (dd, *J* = 5.5, 8.5 Hz, 1H), 7.46 (d, *J* = 9.0 Hz, 1H), 7.41 (dd, *J* = 2.5, 2.5 Hz, 1 h), 6.56 (s, 1H), 5.21–5.08 (m, 1H), 4.60 (s, 1H), 4.03 (br s, 4H), 3.08 (br s, 4H), 3.64–3.53 (m, 2H), 3.47–3.53 (m, 2H), 2.71–2.54 (m, 2H), 2.23–2.11 (m, 2H). MS (ESI): *m/e* 248.1 (24%), 495.3 [M + H]⁺ (100%). HRMS *m/z* 495.261 73, calcd [M + H]⁺ 495.261 54, rel intens 100%, error 0.19 mAmu.

6-(1*H*-Indol-5-yl)-4-morpholin-4-yl-1-[1-(pyridin-3-ylcarbonyl)-piperidin-4-yl]-1*H*-pyrazolo[3,4-*d*]pyrimidine (5v). Procedure C was used. Purification was by preparative reverse phase HPLC with 0.02% ammonium hydroxide buffer, giving an off-white amorphous solid. ¹H NMR (300 MHz, DMSO-*d*₆): δ 11.26 (s, 1H), 8.74–8.65 (m, 2H), 8.31–8.26 (m, 2H), 7.94–7.88 (m, 1H), 7.66–7.50 (m, 4H), 6.56 (s, 1H), 5.21–5.11 (m, 1H), 4.69–4.59 (m, 1H), 4.06–3.99 (m, 1H), 3.84–3.77 (m, 4H), 3.31–3.12 (m, 3H), 2.41–1.90 (m, 4H). MS (ESI): *m/e* 279.1 (19%), 509.2 [M + H]⁺ (100%). HRMS *m/z* 509.241 37, calcd [M + H]⁺ 509.240 80, rel intens 100%, error 0.57.

HPLC Data for 5a–v. Table 4 lists the HPLC retention times and purities for 5a–v.

Assays of mTOR, PI3K, and Other Kinases. mTOR assays were performed in 96-well plates for 2 h at room temperature in 25 μL containing 6 nM Flag-TOR(3.5), 1 μM His6-S6K1, and 100 μM ATP. The assays were performed and detected by DELFIA employing an Eu-phospho-p70S6K T389 antibody as described previously.³⁰ For inhibitor versus ATP matrix competition, mTOR kinase reactions were carried out with varying concentrations of ATP in combination with varying concentrations of inhibitor. The assays contained 12 nM Flag-TOR(3.5) and were incubated for 30 min. The assay results were similarly detected by DELFIA and processed for generation of double-reciprocal plots. PI3K assays were performed in a fluorescence polarization (FP) assay with 25 μM ATP as described.³¹ The assays of 5u (2 μM) against a broad panel of protein kinases were performed by Invitrogen SelectScreen profiling.²⁷

Inhibition of Cellular mTOR Signaling. Human A498 renal cancer and U87MG glioma cells were cultured employing standard cell culture methods, treated with DMSO or inhibitors for 6 h. Total cell lysates were prepared using NuPAGE-LDS sample buffer (Invitrogen), quantified, and subject to immunoblotting analysis using NuPAGE electrophoresis system (Invitrogen). Antibodies against P-S6K1 (T389), P-4EBP1 (T70), P-4EBP1 (T37/46), P-AKT (S473), and P-AKT (T308) were purchased from Cell Signaling Technology.

Molecular Modeling. An mTOR homology model was built based on an in-house PI3K-γ crystal structure in complex with a compound from the pyrazolopyrimidine series. The structure has a resolution of 2.8 Å and an *R*_{free} of 0.28. The structure has been made publicly available through the Protein Data Bank (www.rcsb.org) with identifier 3IBE. PRIME 1.5 (Prime, version 1.5, Schrödinger, LLC, New York, NY, 2005) was used to

Table 4. HPLC Retention Times and Purity Data for 5a–v

compd	method A ^a		method B ^b	
	<i>t</i> _R (min)	purity (%)	<i>t</i> _R (min)	purity (%)
5a	1.86	95	1.25	95
5b	2.34	95	1.28	96
5c	2.07	95	2.81	99
5d	2.33	95	1.38	99
5e	2.12	97	2.34	99
5f	1.90	100	1.85	98
5g	2.26	100	2.91	100
5h	2.08	96	2.25	97
5i	1.92	98	2.21	95
5j	1.87	100	2.29	94
5k	2.26	95	3.51	99
5l	2.13	99	2.57	98
5m	2.00	95	1.93	95
5n	2.16	99	2.51	99
5o	2.26	90	2.47	95
5p	2.15	100	2.54	100
5q	2.31	98	2.65	94
5r	2.12	95	2.50	97
5s	2.37	99	2.84	99
5t	2.04	100	1.66	100
5u	2.02	100	1.80	92
5v	2.45	95	1.77	96

^aHPLC method A: solvent gradient = 90% A at 0 min, 5% A at 2.6 min, 5% A at 3 min; solvent A = 0.05% HCO₂H in water; solvent B = 0.05% HCO₂H in ACN; flow rate = 1 mL/min; column = Agilent XDB-C18 30 mm × 2.1 mm, 1.8 μm particle size; temperature = 70 °C.

^bHPLC method B: 90% A at 0 min, 5% A at 2.6 min, 5% A at 3 min; solvent A = 0.05% NH₄OH in water; solvent B = 0.05% NH₄OH in ACN; flow rate = 1 mL/min; column = Agilent SB-C18, 50 mm × 2.1 mm, 1.8 μm particle size; temperature = 70 °C.

build the initial model, which was further optimized using EMBRACE (MacroModel, version 9.1, Schrödinger, LLC, New York, NY, 2005) minimizations in complex with the cocrystallized ligand. Subsequent docking studies were performed using Glide 4.0 (Glide, version 4.0, Schrödinger, LLC, New York, NY, 2005) and 4.5 (Glide, version 4.5, Schrödinger, LLC, New York, NY, 2005) with the Single Precision (SP) scoring function and a pregenerated docking grid. The box size used for docking was 10 Å in each direction around the centroid of the ligand. To minimize the conformational search space, a hydrogen bonding constraint to valine-2240 of the hinge region was used during the docking.

Acknowledgment. We thank the Wyeth HTS group for mTOR HTS, Xidong Feng for HRMS data, Michael Kelly for HPLC purity analyses, Frank Loganzo for kinase panel assay results, Li Di for rat hepatocytes clearance measurements, and Tarek S. Mansour, Dennis Powell, and Semiramis Ayral-Kaloustian for helpful suggestions.

Note Added after ASAP Publication. This paper was published on October 19, 2009 with an incomplete author list. The revised version was published on October 22, 2009.

References

- (1) Sarbassov, D. D.; Ali, S. M.; Sabatini, D. M. Growing role of the mTOR pathway. *Curr. Opin. Cell Biol.* **2005**, *17*, 596–603.
- (2) Wullschleger, S.; Loewith, R.; Hall, M. N. TOR signaling in growth and metabolism. *Cell* **2006**, *124*, 471–484.
- (3) Guertin, D. A.; Sabatini, D. M. Defining the role of mTOR in cancer. *Cancer Cell* **2007**, *12*, 9–22.
- (4) Chiang, G. G.; Abraham, R. T. Targeting the mTOR signaling network in cancer. *Trends Mol. Med.* **2007**, *13*, 433–442.
- (5) Guertin, D. A.; Sabatini, D. M. The pharmacology of mTOR inhibition. *Sci. Signaling* **2009**, *2*, 1–6.

- (6) Abraham, R. T. PI 3-kinase related kinases: "big" players in stress-induced signaling pathways. *DNA Repair* **2004**, *3*, 883–887.
- (7) Yuan, T. L.; Cantley, L. C. PI3K pathway alterations in cancer: variations on a theme. *Oncogene* **2008**, *27*, 5497–5510.
- (8) Carracedo, A.; Pandolfi, P. P. The PTEN-PI3K pathway: of feedbacks and cross-talks. *Oncogene* **2008**, *27*, 5527–5541.
- (9) Inoki, K.; Corradetti, M. N.; Guan, K. L. Dysregulation of the TSC-mTOR pathway in human disease. *Nat. Genet.* **2005**, *37*, 19–24.
- (10) Choi, J.; Chen, J.; Schreiber, S. L.; Clardy, J. Structure of the FKBP12–rapamycin complex interacting with the binding domain of human FRAP. *Science* **1996**, *273*, 239–242.
- (11) Liang, J.; Choi, J.; Clardy, J. Refined structure of the FKBP12–rapamycin–FRB ternary complex at 2.2 Å resolution. *Acta Crystallogr., Sect. D: Biol. Crystallogr.* **1999**, *55*, 736–744.
- (12) Easton, J. B.; Houghton, P. J. mTOR and cancer therapy. *Oncogene* **2006**, *25*, 6436–6446.
- (13) Dancy, J. E. Therapeutic targets: MTOR and related pathways. *Cancer Biol. Ther.* **2006**, *5*, 1065–1073.
- (14) Abraham, R. T.; Gibbons, J. J. The mammalian target of rapamycin signaling pathway: twists and turns in the road to cancer therapy. *Clin. Cancer Res.* **2007**, *13*, 3109–3114.
- (15) Sarbassov, D. D.; Ali, S. M.; Kim, D. H.; Guertin, D. A.; Latek, R. R.; Erdjument-Bromage, H.; Tempst, P.; Sabatini, D. M. Rictor, a novel binding partner of mTOR, defines a rapamycin-insensitive and raptor-independent pathway that regulates the cytoskeleton. *Curr. Biol.* **2004**, *14*, 1296–1302.
- (16) Jacinto, E.; Loewith, R.; Schmidt, A.; Lin, S.; Ruegg, M. A.; Hall, A.; Hall, M. N. Mammalian TOR complex 2 controls the actin cytoskeleton and is rapamycin insensitive. *Nat. Cell Biol.* **2004**, *6*, 1122–8.
- (17) Carracedo, A.; Ma, L.; Teruya-Feldstein, J.; Rojo, F.; Salmena, L.; Alimonti, A.; Egia, A.; Sasaki, A. T.; Thomas, G.; Kozma, S. C.; Papa, A.; Nardella, C.; Cantley, L. C.; Baselga, J.; Pandolfi, P. P. Inhibition of mTORC1 leads to MAPK pathway activation through a PI3K-dependent feedback loop in human cancer. *J. Clin. Invest.* **2008**, *118*, 3065–3074.
- (18) Sauveur-Michel, M.; Stauffer, F.; Brueggen, J.; Furet, P.; Schnell, C.; Fritsch, C.; Brachmann, S.; Chene, P.; De Pover, A.; Schoemaker, K.; Fabbro, D.; Gabriel, D.; Simonen, M.; Murphy, L.; Finan, P.; Sellers, W.; Garcia-Echeverria, C. Identification and characterization of NVP-BEZ235, a new orally available dual phosphatidylinositol 3-kinase/mammalian target of rapamycin inhibitor with potent in vivo antitumor activity. *Mol. Cancer Ther.* **2008**, *7*, 1851–1863.
- (19) Raynaud, F. I.; Eccles, S.; Clarke, P. A.; Angela, H.; Bernard, N.; Sonia, A.; Henley, A.; Di-Stefano, F.; Ahmad, Z.; Guillard, S.; Bjerke, L. M.; Kelland, L.; Valenti, M.; Patterson, L.; Gowan, S.; De Haven Brandon, A.; Hayakawa, M.; Kaizawa, H.; Koizumi, T.; Ohishi, T.; Patel, S.; Saghir, N.; Parker, P.; Waterfield, M.; Workman, P. Pharmacologic characterization of a potent inhibitor of class I phosphatidylinositide 3-kinases. *Cancer Res.* **2007**, *67*, 5840–5850.
- (20) Folkes, A. J.; Ahmadi, K.; Alderton, W. K.; Alix, S.; Baker, S. J.; Box, G.; Chuckowree, I. S.; Clarke, P. A.; Depledge, P.; Eccles, S. A.; Friedman, L. S.; Hayes, A.; Hancox, T. C.; Kugendradas, A.; Lensun, L.; Moore, P.; Olivero, A. G.; Pang, J.; Patel, S.; Pergl-Wilson, G. H.; Raynaud, F. I.; Robson, A.; Saghir, N.; Salphati, L.; Sohal, S.; Ultsch, M. H.; Valenti, M.; Wallweber, H. J. A.; Wan, N. C.; Wiesmann, C.; Workman, P.; Zhyvoloup, A.; Zvelebil, M. J.; Shuttleworth, S. J. The identification of 2-(1*H*-indazol-4-yl)-6-(4-methanesulfonyl-piperazin-1-ylmethyl)-4-morpholin-4-yl-thieno[3,2-*d*]pyrimidine (GDC-0941) as a potent, selective, orally bioavailable inhibitor of class I PI3 kinase for the treatment of cancer. *J. Med. Chem.* **2008**, *51*, 5522–5532.
- (21) Yu, K.; Toral-Barza, L.; Shi, C.; Zhang, W.-G.; Lucas, J.; Shor, B.; Kim, J.; Verheijen, J.; Curran, K.; Malwitz, D. J.; Cole, D. C.; Ellingboe, J.; Ayral-Kaloustian, S.; Mansour, T. S.; Gibbons, J. J.; Abraham, R. T.; Nowak, P.; Zask, A. Biochemical, cellular and in vivo activity of novel ATP-competitive and selective inhibitors of the mammalian target of rapamycin. *Cancer Res.* **2009**, *69*, 6232–6240.
- (22) Feldman, M. E.; Apsel, B.; Uotila, A.; Loewith, R.; Knight, Z. A.; Ruggero, D.; Shokat, K. M. Active-site inhibitors of mTOR target rapamycin-resistant outputs of mTORC1 and mTORC2. *PLoS Biol.* **2009**, *7*, 371–383.
- (23) Garcia-Martinez, J. M.; Moran, J.; Clarke, R. G.; Gray, A.; Cosulich, S. C.; Chresta, C. M.; Alessi, D. R. Ku-0063794 is a specific inhibitor of the mammalian target of rapamycin (mTOR). *Biochem. J.* **2009**, *421*, 29–42.
- (24) Thoreen, C. C.; Kang, S. A.; Chang, J. W.; Liu, Q.; Zhang, J.; Gao, Y.; Reichling, L. J.; Sim, T.; Sabatini, D. M.; Gray, N. S. An ATP-competitive mammalian target of rapamycin inhibitor reveals rapamycin-resistant functions of mTORC1. *J. Biol. Chem.* **2009**, *284*, 8023–8032.
- (25) Hopkins, L. A.; Groom, C. R.; Alex, A. Ligand efficiency: a useful metric for lead selection. *Drug Discovery Today* **2004**, *9*, 430–431.
- (26) Keseru, G. M.; Makara, G. M. The influence of lead discovery strategies on the properties of drug candidates. *Nat. Rev. Drug Discovery* **2009**, *8*, 203–212.
- (27) <http://www.invitrogen.com/kinaseprofiling>.
- (28) Matsushita, K.; Hasegawa, H.; Kuribayashi, Y.; Ohashi, N. Preparation of Sulfonylureidopyrazole Derivatives as Endothelin Converter Enzyme Inhibitors. PCT Int. Appl. WO 9730978 A1, **1997**; Sumitomo Pharmaceuticals Co., Ltd., Japan.
- (29) Muller, M. A.; Gaplovsy, M.; Wirz, J.; Woggon, W.-D. Synthesis and photophysical properties of a deazaflavin-bridged porphyrinatoiron(III) that mimics the interaction of a deazaflavin inhibitor with the heme-thiolate cofactor of cytochrome P450 3A4. *Helv. Chim. Acta* **2006**, *89*, 2987–3001.
- (30) Toral-Barza, L.; Zhang, W. G.; Lamison, C.; LaRocque, J.; Gibbons, J.; Yu, K. Characterization of the cloned full-length and a truncated human target of rapamycin: activity, specificity, and enzyme inhibition as studied by a high capacity assay. *Biochem. Biophys. Res. Commun.* **2005**, *332*, 304–310.
- (31) Zask, A.; Kaplan, J.; Toral-Barza, L.; Hollander, I.; Young, M.; Tischler, M.; Gaydos, C.; Cinque, M.; Lucas, J.; Yu, K. Synthesis and structure–activity relationship of ring-opened 17-hydroxywortmannins: potent phosphoinositide 3-kinase inhibitors with improved properties and anticancer efficacy. *J. Med. Chem.* **2008**, *51*, 1319–1323.